minerals
MDPI
Article

Anisotropy of Out-of-Phase Magnetic Susceptibility: A Non-Standard Approach for Magnetic Subfabrics Determination in Variscan Granites of Iberian Massif

Cláudia Cruz [1,2,*], Helena Sant'Ovaia [1,2], William McCarthy [3] and Fernando Noronha [1,2]

1 Departamento de Geociências Ambiente e Ordenamento do Território, Faculdade de Ciências da Universidade do Porto, Rua do Campo Alegre 687, 4169-007 Porto, Portugal
2 Pólo-Porto, Instituto de Ciências da Terra, Rua do Campo Alegre 687, 4169-007 Porto, Portugal
3 Irvine Building St Andrews, School of Earth & Environment Sciences, St Andrews KY16 8LG, UK
* Correspondence: claudiacruz@fc.up.pt

Abstract: The magnetic susceptibility measured in an alternating field is made up of in-phase and out-of-phase components. The in-phase Anisotropy of Magnetic Susceptibility (ipAMS) measures the bulk response of all minerals in a sample; however, out-of-phase AMS (opAMS) is sensitive to only select ferromagnetic minerals such as hematite, titanomagnetite, and ultrafine magnetite. The opAMS can be harnessed as a tool for the direct determination of magnetic subfabrics defined by ferromagnetic minerals. This work focuses on the following three Portuguese plutons: Lamas de Olo, Lavadores-Madalena, and Santa Eulália. The results show that the magnetic susceptibility is lower in opAMS, the degree of magnetic anisotropy is much higher in the opAMS, and the ellipsoid shape parameter has no significant differences. The ipAMS and opAMS tensors are, in general, coaxial, which indicates that the standard AMS fabric is parallel to the subfabric of minerals such as hematite, titanomagnetite, and ultrafine magnetite.

Keywords: anisotropy of out-of-phase magnetic susceptibility; anisotropy of in-phase magnetic susceptibility; rock and mineral magnetism

check for updates

Citation: Cruz, C.; Sant'Ovaia, H.; McCarthy, W.; Noronha, F. Anisotropy of Out-of-Phase Magnetic Susceptibility: A Non-Standard Approach for Magnetic Subfabrics Determination in Variscan Granites of Iberian Massif. *Minerals* **2022**, *12*, 1376. https://doi.org/10.3390/min12111376

Academic Editor: Hans-Rudolf Wenk

Received: 30 September 2022
Accepted: 26 October 2022
Published: 29 October 2022

1. Introduction

The Anisotropy of Magnetic Susceptibility (AMS), also referred to as the standard AMS, represents the composition of minerals in a rock sample; if more than one rock fabric is present, an intermediate AMS tensor may be recorded [1].

Several techniques were developed to isolate the magnetic subfabrics based on the specific behavior and susceptibility of individual minerals in variable magnetic fields or at variable temperatures. Authors such as Hrouda and Jelinek [2], Rochette et al. [3], Martín-Hernandez and Hirt [4], Ferré et al. [5], Román-Berdiel et al. [6], Raposo and Gastal [7], and Oliva-Urcia et al. [8], among others, used techniques to separate the magnetic subfabrics of diamagnetic and paramagnetic minerals. On the other hand, other techniques can help in separating the magnetic subfabrics of pyrrhotite/hematite from the paramagnetic mineral subfabric (e.g., [5,9,10]).

Hrouda et al. [11–13] developed a method which utilized the anisotropy of out-of-phase magnetic susceptibility for the direct determination of magnetic subfabrics, as well as the magnetic granulometry of some minerals. This technique is based on the perception that when measuring susceptibility in a low alternating magnetic field, the measured specimen is usually magnetized by a weak field sinusoidally varying in time, and its magnetic response is measured. The AMS measured in the alternating field can be divided into two components: (i) one which is in-phase with the applied field, and (ii) another which is out-of-phase with the applied field. In the component that is in-phase with the applied field, the response occurs instantaneously and produces a zero-phase angle; this is typical of non-conductive diamagnetic, paramagnetic, and many ferromagnetic sensus latus (s.l.) materials (e.g., multidomain magnetite). Conversely, in a component that is out-of-phase, the magnetization is not in-phase with the applied field but lags behind the field to produce a non-zero phase angle [11–14].

Rocks are usually composed of diamagnetic, paramagnetic, and ferromagnetic s.l. minerals. Therefore, in anisotropic materials, such as rocks, the magnetic susceptibility (k) is also anisotropic and can be subdivided into the following two components: (i) one in-phase with the applied field (ipK_m), and (ii) the other out-of-phase (opK_m). Accordingly, the anisotropies of these components can be defined as in-phase magnetic anisotropy (ipAMS) and out-of-phase anisotropy (opAMS) [12,14]. The ipAMS is the standard AMS (e.g., [15,16]) whereas the measurement of the opAMS is more difficult and its technique was only developed recently by Hrouda et al. [11–14].

Only some ferromagnetic viscous minerals exhibit an out-of-phase response; these include hematite, titanomagnetite, and ultrafine grains of magnetite. There are three major physical mechanisms that produce the opK_m [16]:

Viscous relaxation is typical of ultrafine magnetic particles, such as ultrafine grains of magnetite that are between the blocked and unblocked states at a superparamagnetic (SP)/stable single domain (SSD) boundary;

(i) Electrical eddy currents (induced by an AC field in conductive materials) are characteristic of minerals that are at least moderately conductive electrically;
(ii) Weak field hysteresis (non-linear and irreversible dependence of M on H) is typical of minerals that show a wide hysteresis loop, such as titanomagnetite, pyrrhotite, and hematite.

The presence of magnetite in Iberian granites has been described in several works, both in Portugal and in Spain (e.g., [6,17–24]). Nevertheless, the occurrence of magnetite-type granites [25] is rare and only the following five occurrences are known in Portugal: Peneda-Gerês, Lamas de Olo, and Lavadores-Madalena plutons in the north [17,18]; Manteigas granodiorite in the center [19]; and Santa Eulália Plutonic Complex in south Portugal [20].

The purpose of this work is to enhance and complement previous studies [21] of the magnetic subfabrics of three Portuguese magnetite-type plutons and to verify if minerals, such as magnetite and hematite, have the same orientation as the other minerals present in these plutons. The plutons studied are Lamas de Olo, Lavadores-Madalena, and Santa Eulália.

2. Materials and Methods

2.1. Fundamentals of Out-of-Phase Magnetic Susceptibility

To measure the magnetic susceptibility in a low alternating magnetic field, the samples are magnetized by a weak field sinusoidally varying in time (Equation (1)) (e.g., [13]):

$$H(t) = H_0 \cos(\omega t) \tag{1}$$

where H_0 represents amplitude, ω is the angular frequency, and t is time; the magnetic response is represented by magnetization, *M(t)* (Equation (2)) (e.g., [13]).

$$M(t) = M_0 \cos[\omega(t - \Delta t)] = M_0 \cos(\omega t - \delta) \tag{2}$$

where M_0 is amplitude, Δt represents the time lag, ω is the angular frequency, and δ refers to the phase.

In such materials, the susceptibility is determined for the in-phase (ipK_m) and out-of-phase (opK_m) components, and the phase angle δ, which expresses the strength of the opAMS response, was defined as (Equation (3)) (e.g., [13]):

$$\tan \delta = \frac{opK_m}{ipK_m} \tag{3}$$

2.2. Analytical Techniques and Calculated Parameters

For the present study, 22 mm long × 24 mm diameter cylindrical sub-samples (ca. 10 cm^3) of three different Variscan granites were examined. The ipAMS and opAMS were measured with the KLY5-A Kappabridge from AGICO, Inc., Brno, Czech Republic, using a fully automated 3D rotator from the *Magnetics, Minerals, Magma and Ore "M3Ore" Laboratory* at the University of St. Andrews in a low alternating field of 400 A/m at 1.22 kHz, at room temperature. The AMS ellipsoid for each sub-sample was calculated from the magnetic susceptibility data obtained using Anisoft 4 [26]. The mean of all the sub-specimens from each sample site was calculated with Anisoft 4 to determine the site-averaged AMS ellipsoids.

The ipAMS and opAMS were determined simultaneously, and the calculus for the computation of the opAMS is the same as that for the computation of the ipAMS. It should be noted that the measurements were collected using the x, y, and z coordinate system.

The obtained data help to establish the magnetic susceptibility tensor, represented by a triaxial ellipsoid. The intensities and orientations of the three axes, $K_1 \geq K_2 \geq K_3$, and the 95% confidence angles, E_{12}, E_{23}, and $E_{31,}$ corresponding to these axes were calculated. The ratios between the *K* axes' magnitudes provide several magnetic parameters [16,27], such as:

(i) Mean susceptibility (Equation (4)):

$$K_m = \frac{K_1 + K_2 + K_3}{3} \tag{4}$$

(ii) Degree of magnetic anisotropy (Equation (5)):

$$P_j = \exp\sqrt{2[(n_1 - n)^2 + (n_2 - n)^2 + (n_3 - n)^2]} \tag{5}$$

(iii) Shape ellipsoid (Equation (6)):

$$Tj = 2\left[\left(\frac{ln\ (K_2/K_3)}{ln\ (K_1/K_2)}\right) - 1\right] \tag{6}$$

where $K_1 > K_2 > K_3$ are principal susceptibilities, and $n = (n_1 + n_2 + n_3)/3$, and n_1, n_2, and n_3 are their respective natural logarithms.

3. Geological Setting

3.1. Regional Context

The Iberian Variscan belt is a large, curved section of the European Variscan belt that resulted from the collision between two supercontinents, the Laurussia and Gondwana, during the Devonian and Carboniferous periods [28–30].

The Iberian Variscan belt is divided into the following geotectonic zones: the Cantabrian Zone, the West Asturian Leonese Zone, the Central Iberian Zone (CIZ), the Ossa-Morena Zone (OMZ), and the South Portuguese Zone [27]. This work focuses on the CIZ, and OMZ [31].

3.2. Studied Plutons

The present study investigated the following three Portuguese Variscan composite plutons (Figure 1): (i) the Lamas de Olo Pluton (LOP), (ii) the Lavadores-Madalena Pluton (LMP), and (iii) the Santa Eulália Plutonic Complex (SEPC).

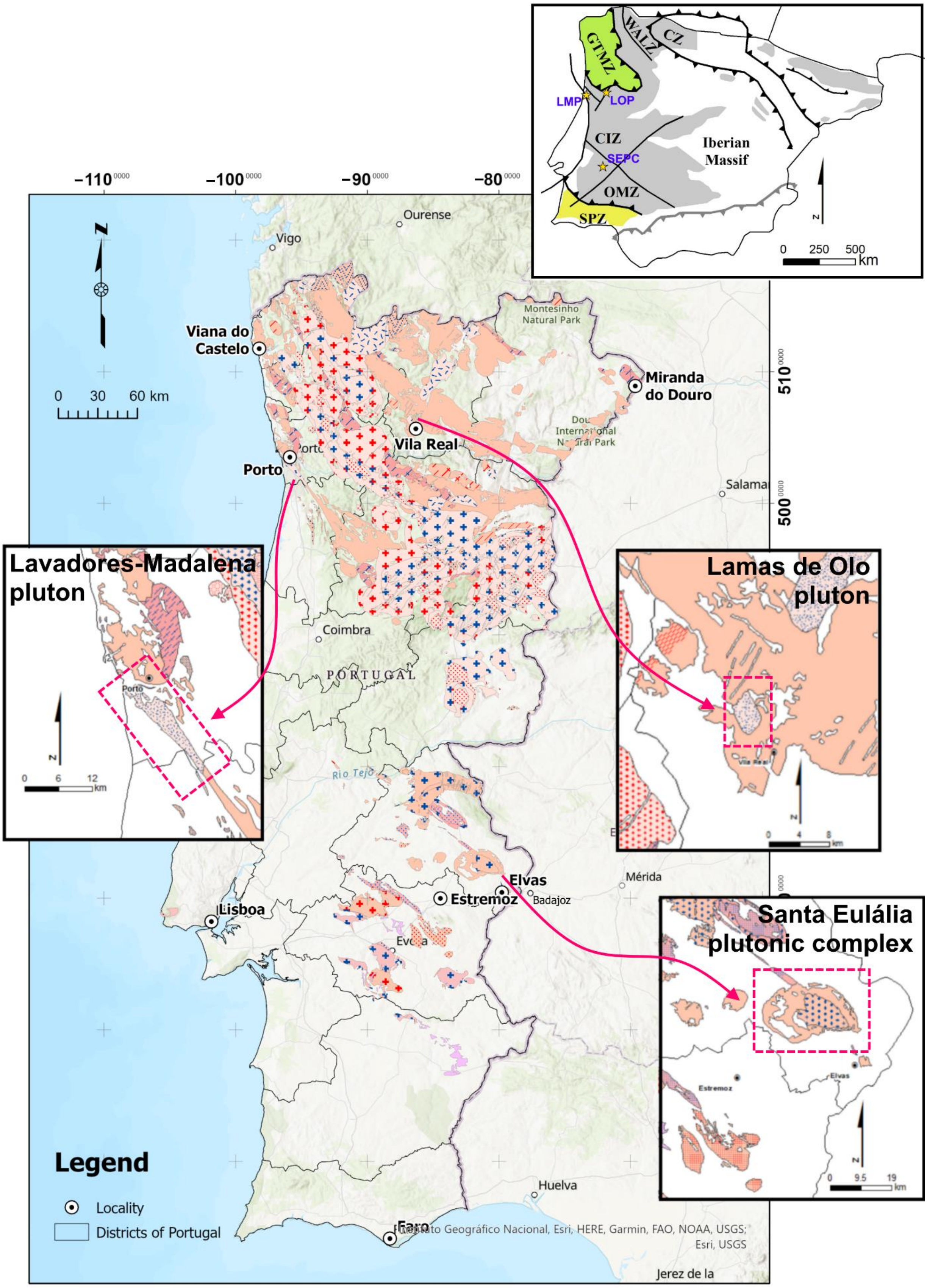

Figure 1. Location of the studied areas in the Iberian Peninsula, and a simplified geological map of studied plutons (Lamas de Olo pluton, Lavadores-Madalena pluton, Santa Eulália Plutonic Complex).

All the plutons are post-kinematic, Late Carboniferous–Early Permian in age and have magnetite in their composition. The LOP and LMP are located in the Central-Iberian Zone (CIZ), north and northwest of Portugal, respectively, and the SEPC outcrops in the Ossa-Morena Zone (OMZ), southeast of Portugal, near the contact between CIZ and OMZ [32].

The Lamas de Olo Pluton (LOP) is a post-tectonic body located in the northern part of CIZ at the Iberian Variscan belt. The LOP is a composite pluton composed of distinct granites that are similar in mineralogical composition but with different grain sizes, namely the: (i) Lamas de Olo, (ii) Alto dos Cabeços, and (iii) Barragem granites. The main granite is the Lamas de Olo, which is characterized by a medium-to coarse-grained porphyritic granite. The Alto dos Cabeços is a fine- to medium-grained, porphyritic granite. The younger granite that cuts the other two granites is Barragem, which outcrops in the center of the pluton, near the dam; it is classified as leucocratic, fine- to medium-grained and slightly porphyritic granite. LOP granites are mostly composed of quartz, plagioclase, K-feldspars, and biotite. Muscovite I, muscovite II, zircon, sphene, allanite, fluorite, hematite, magnetite, ilmenite, chlorite, rutile, apatite, goethite, epidote, and tourmaline are present as accessory minerals [18,33–36]. Available geochronologic Pb/U data indicate an age of ca. 297 Ma for the Lamas de Olo granite [35]. The magnetic susceptibility values show a heterogeneous behavior across the pluton (21 μSI < K_m < 44,382 μSI). The Lamas de Olo granite shows a higher variability in magnetic susceptibility values, and the Barragem granite has lower magnetic susceptibility mean values (Figure 2). The K_m data, combined with petrographic and other magnetic mineralogy studies (e.g., thermomagnetic curves and the treatment of isothermal remanence magnetization data by the cumulative log-Gaussian function), suggest that the LOP is composed of magnetite-type granites but areas of magnetic- and non-magnetic-behavior are also present [18,36,37]. Previous studies [18] show that the LOP has a complex magnetic mineralogy, with both hematite and magnetite. However, in the Alto dos Cabeços granite, most of the magnetite is altered into hematite (martite), and in the Barragem granite, although magnetite is not observed under a microscope, it was identified in minor amounts through the thermomagnetic curves and the isothermal remanence magnetization curves [18].

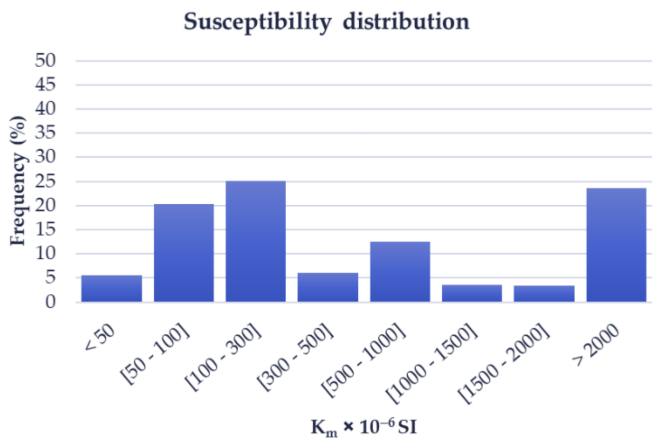

(**a**)

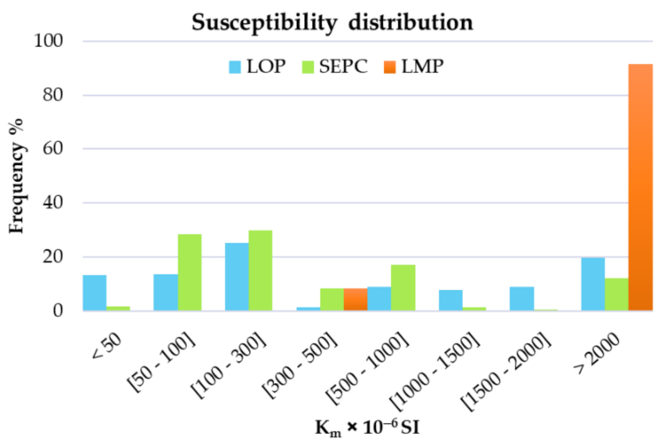

(**b**)

Figure 2. Relative frequency magnetic susceptibility histograms: (**a**) for all the studied granites; (**b**) for the plutons; LOP: Lamas de Olo Pluton; SEPC: Santa Eulália Plutonic Complex; LMP: Lavadores-Madalena Pluton (total of measured samples = 1162).

The Lavadores-Madalena Pluton (LMP) is located in CIZ, in northwest Portugal (near Porto). The LMP is dated ca. 298 Ma [38] and is composed of the following two granites: (i) Lavadores, and (ii) Madalena. The Lavadores granite is a porphyritic, coarse-grained biotite granite and contains quartz, plagioclase, perthitic orthoclase and microcline, biotite, magnetite, hematite, zircon, sphene, apatite, allanite, and amphibole [38]. The Madalena is a porphyritic, medium- to coarse-grained biotite granite composed of quartz, orthoclase, plagioclase, biotite, magnetite, hematite, zircon, apatite, muscovite, and chlorite [17]. Studies of magnetic susceptibility and isothermal remnant magnetization of the Lavadores-Madalena pluton demonstrate that it is a magnetite-type (Figure 2). The magnetic susceptibility values are in the range of 7130×10^{-6} SI < K_m < $19{,}303 \times 10^{-6}$ SI [17,38]. Thermomagnetic curves show the presence of magnetite/Ti-poor magnetite and hematite [18].

The Santa Eulália Plutonic Complex (SEPC) is composed of the following two concentric granites: (i) G0 granite, and (ii) G1 granite. The external granite is G0 and it consists of a medium- to coarse-grained pink granite. This granite is mostly composed of quartz, biotite, K-feldspar, and plagioclase, with minor amounts of magnetite, hematite, chlorite, amphibole, allanite, and zircon. The central granite, named G1 granite, is a porphyritic, gray, medium-grained, biotite granite. The mineral assemblage of G1 includes quartz, biotite, plagioclase, microcline, muscovite, and cordierite; however, magnetite is not observed [20,39]. The geochronology U-Pb zircon data defined comparable crystallization ages of 301 ± 0.9 Ma, and 302 ± 2.9 Ma for the G0 and G1 granites, respectively [39]. The magnetic susceptibility data demonstrate that G0 and G1 granites have a different magnetic behavior. G0 is considered a magnetite-type granite, having K_m values between 41.6×10^{-6} SI and 7343.7×10^{-6} SI, and G1 is an ilmenite-type granite, with lower K_m values, between 55.1×10^{-6} SI and 133.7×10^{-6} SI [20] (Figure 2). The formation of G0 required oxidized conditions related to the interaction of mafic rocks with felsic magma.

Petrographic studies of these three plutons show the presence of martitization processes that lead us to conclude that these plutons are magnetite-type granites, but oxidation processes, partially or totally, alter the magnetite into hematite, explaining the lower values in some areas [18,20,39].

4. Results and Discussion

The ipAMS and opAMS data for each sampling site for the Lamas de Olo (LOP), Lavadores-Madalena (LMP), and Santa Eulália (SEPC) plutons are determined (Tables 1 and 2, and Figure 3).

Table 1. ipAMS data for studied granites (n—number of samples; the ipAMS measurements were performed according to a specimen coordinate system).

Pluton	Sampling Site	n	ipAMS										
			Km ($\times 10^{-3}$)	Km ($\times 10^{-6}$)	Pj	Tj	K1 Dec	K1 Inc	K3 Dec	K3 Inc	E12	E23	E31
LOP	LM 19	8	1.77	1765	1.06	0.16	133	43	229	6	42	27	10
	LM 32	8	2.02	2018	1.07	−0.01	48	9	315	20	16	21	36
	LM 33	7	0.00	2	1.73	−0.23	103	69	236	15	39	29	12
	LM 34	6	0.10	99	1.01	0.03	5	3	269	65	11	30	7
	LM 39	8	0.08	83	1.01	0.00	189	22	73	47	35	40	19
LMP	LV 1	8	16.20	16,200	1.16	0.38	106	69	318	18	42	16	17
	LV 4	8	8.41	8410	1.31	0.46	12	30	265	27	72	11	29
SEPC	ASM 076	9	1.85	1851	1.07	0.08	105	31	14	2	37	20	16

The opK_m is much lower than the ipK_m (Figure 3a–c) and the P_j parameter is higher in the opAMS measurements than in the ipAMS measurements (Figure 3a,d); there are also no significant differences in the T_j parameters (Figure 3b,d) due to them consisting of mostly oblate ellipsoids. The phase angle is non-zero in all samples (Table 2; Figure 3c).

Table 2. opAMS data for studied granites and phase angle (the opAMS measurements were performed according to a specimen coordinate system).

Pluton	Sampling Site	opAMS											Phase (°)
		Km ($\times 10^{-3}$)	Km ($\times 10^{-6}$)	Pj	Tj	K1 Dec	K1 Inc	K3 Dec	K3 Inc	E12	E23	E31	
LOP	LM 19	0.0010	0.9501	1.59	0.27	140	76	235	1	21	53	12	0.03
	LM 32	0.0014	1.4491	2.44	0.20	56	48	313	11	74	10	37	0.04
	LM 33	0.0017	1.7471	1.73	−0.23	105	72	227	10	40	72	13	0.06
	LM 34	0.0003	0.3340	1.36	−0.15	16	18	238	66	53	23	32	0.19
	LM 39	0.0011	1.1353	1.40	0.03	61	42	302	28	6	54	6	0.79
LMP	LV 1	0.0481	48.0875	2.77	0.29	96	68	325	15	51	23	22	0.17
	LV 4	0.0085	8.4950	5.24	0.50	60	66	267	22	45	31	10	0.06
SEPC	ASM 076	0.0001	0.1157	30.73	0.24	83	70	186	5	11	37	7	0.01

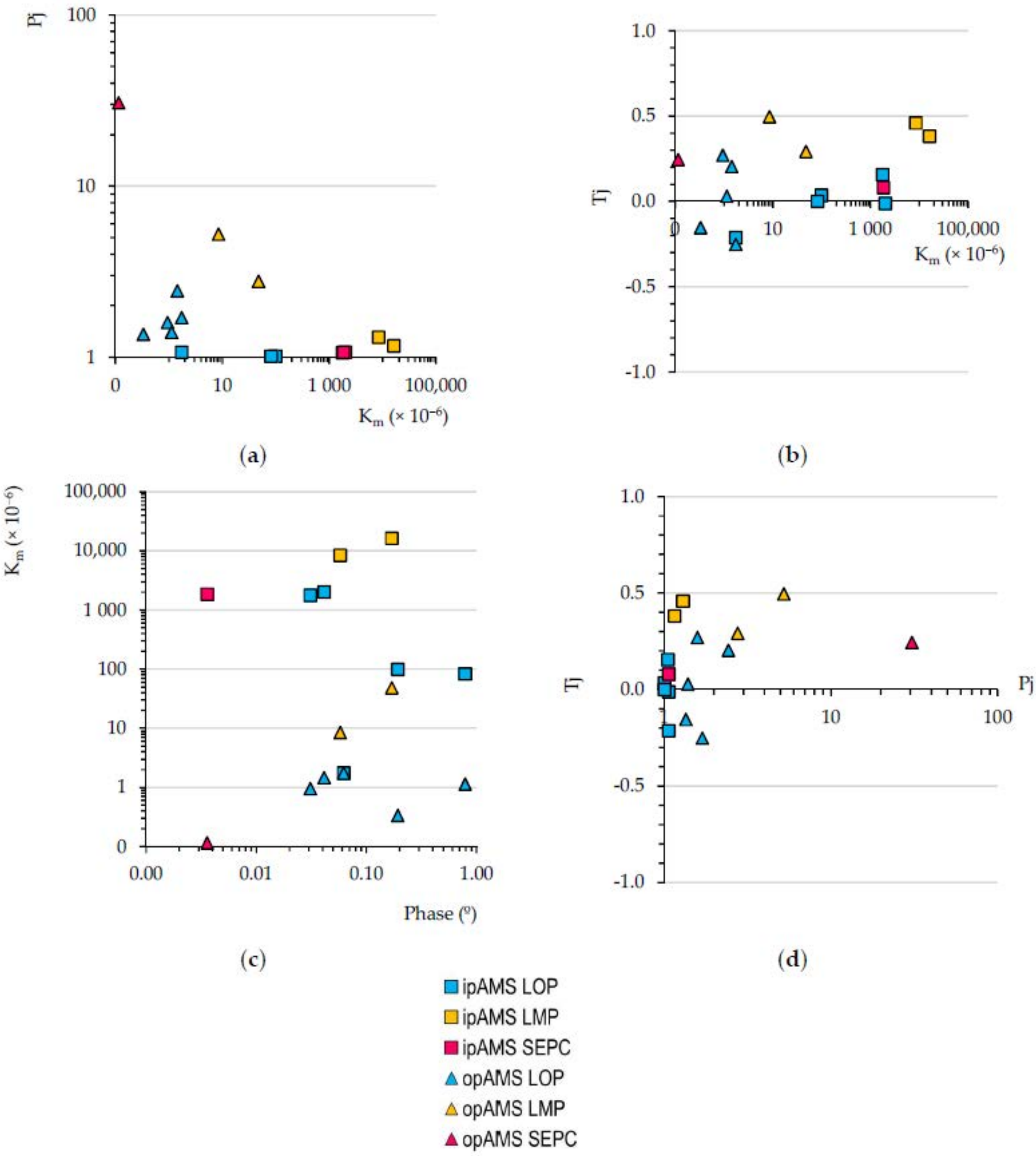

Figure 3. (**a**) P_j vs. K_m plot; (**b**) Tj vs. Pj plot; (**c**) T_j vs. K_m plot; (**d**) K_m vs. phase angle (ipAMS—in-phase AMS; opAMS—out-of-phase AMS); LOP—Lamas de Olo pluton; LMP—Lavadores-Madalena pluton; SEPC—Santa Eulália Plutonic Complex).

An interpretation of the presence of the lower *opK*$_m$ values, when compared with the ip*K*$_m$ values, is that the lower *opK*$_m$ is due to only some minerals being present, which indicates the susceptibility of viscous particles in the transition between superparamagnetic (SP) and stable single domain (SSD) states. In contrast, the *ipK*$_m$ is controlled not only by these grains, but also by the multidomain (MD) grains, and by paramagnetic grains. The frequency dependence of magnetic susceptibility (KfD%) was previously measured in samples from the LOP [18], revealing the presence of superparamagnetic minerals in some areas of the pluton.

The increase in P_j in the opAMS is explained by the grain degree of the opAMS being higher in the ultrafine magnetically viscous particles than the degree of the ipAMS in the MD particles, and also by the possible effect of paramagnetic minerals in the ipAMS.

The *T* parameters are mostly oblate in both the ipAMS and opAMS, which can be interpreted as the main influence of hematite grain anisotropy and magnetite shape anisotropy.

Figures 4 and 5 show that the ipAMS and opAMS tensors are coaxial, except for one site of the LOP (the site LM 39). This site has low *ipK*$_m$ values (Table 1) which indicates the presence of minor amounts of ferromagnetic minerals compared to the other sites. The coaxial tensors reflect the fact that the standard ipAMS fabric is the same as the subfabric of minerals such as hematite, titanomagnetite, and ultrafine magnetite. Even in site LM 34, which has low *ipK*$_m$ values, the tensors are coaxial, indicating the presence of minerals such as hematite (after magnetite) but with the same orientation as the matrix. The occurrence of martitization processes (partial and/or total oxidation of magnetite into hematite) was described in previous works, namely in [18]. On the other hand, the LM 39 site has the K_1 and K_3 orientated differently in the ipAMS and opAMS, suggesting the presence of a ferromagnetic oxide, such as hematite, but with a different orientation to the paramagnetic minerals.

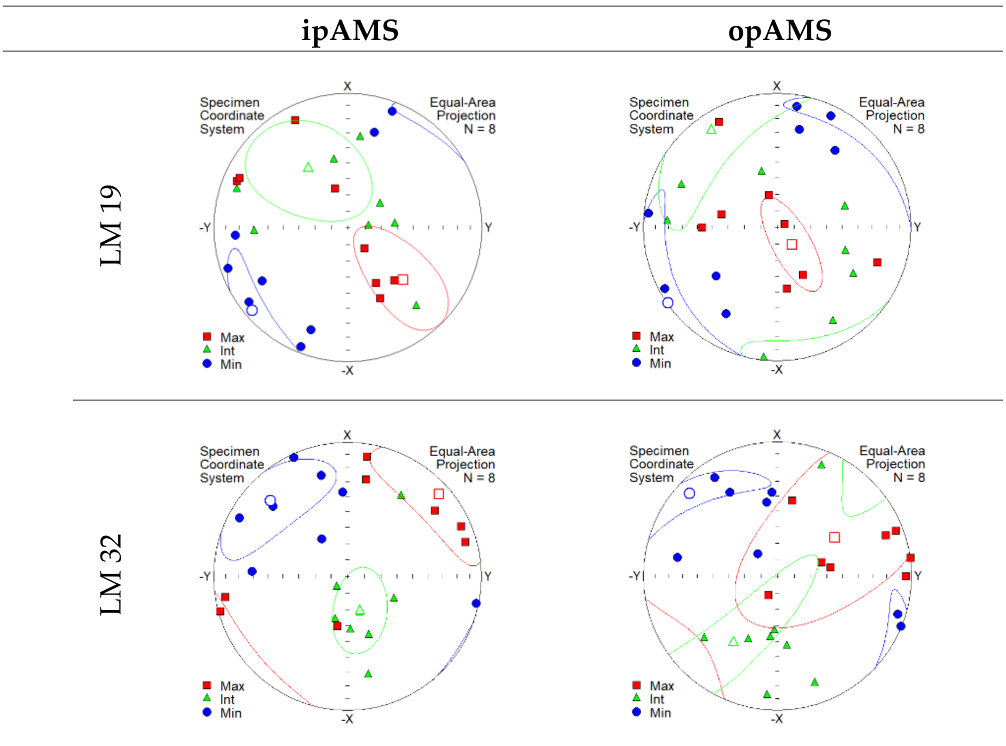

Figure 4. *Cont.*

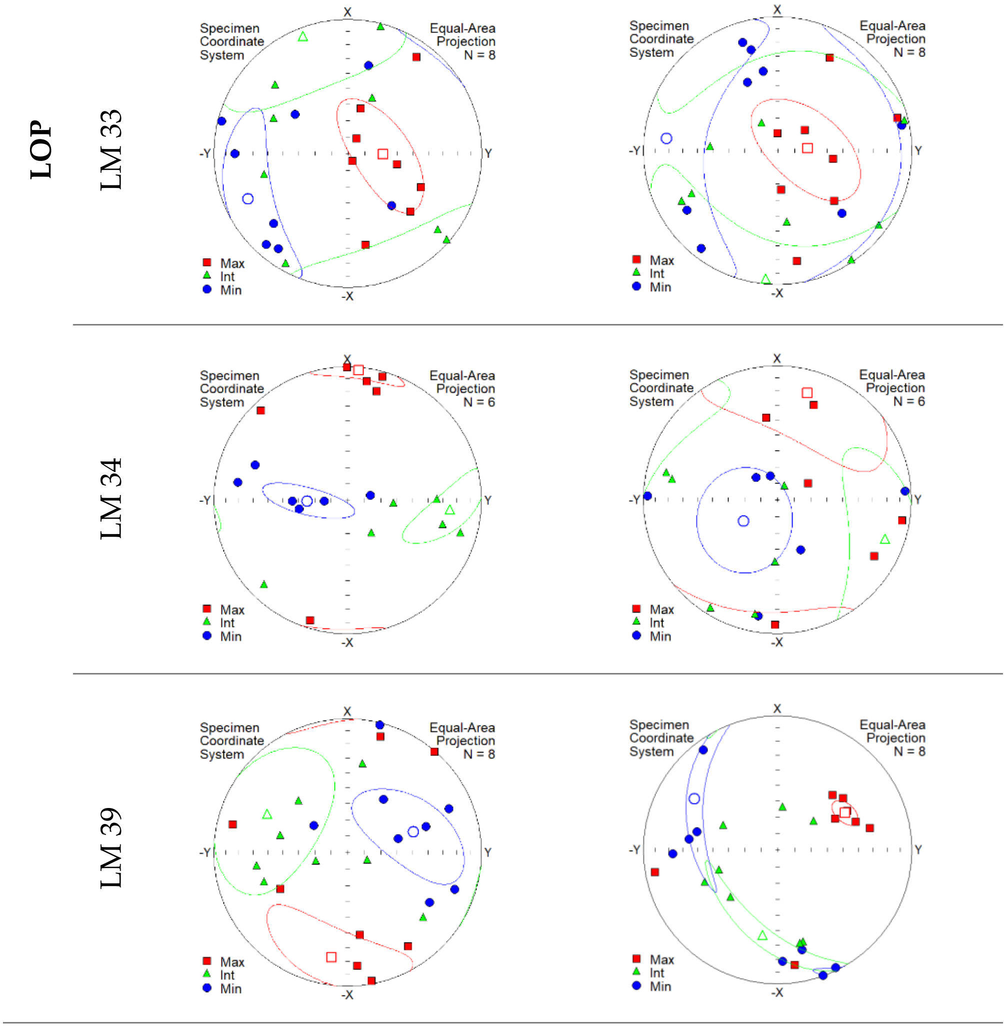

Figure 4. ipAMS and opAMS mean tensors for LOP sub-samples, according to specimen coordinate system, and 95% confidence areas. Equal-area projection, lower hemisphere (the hollow symbols represents the corresponding mean vectors).

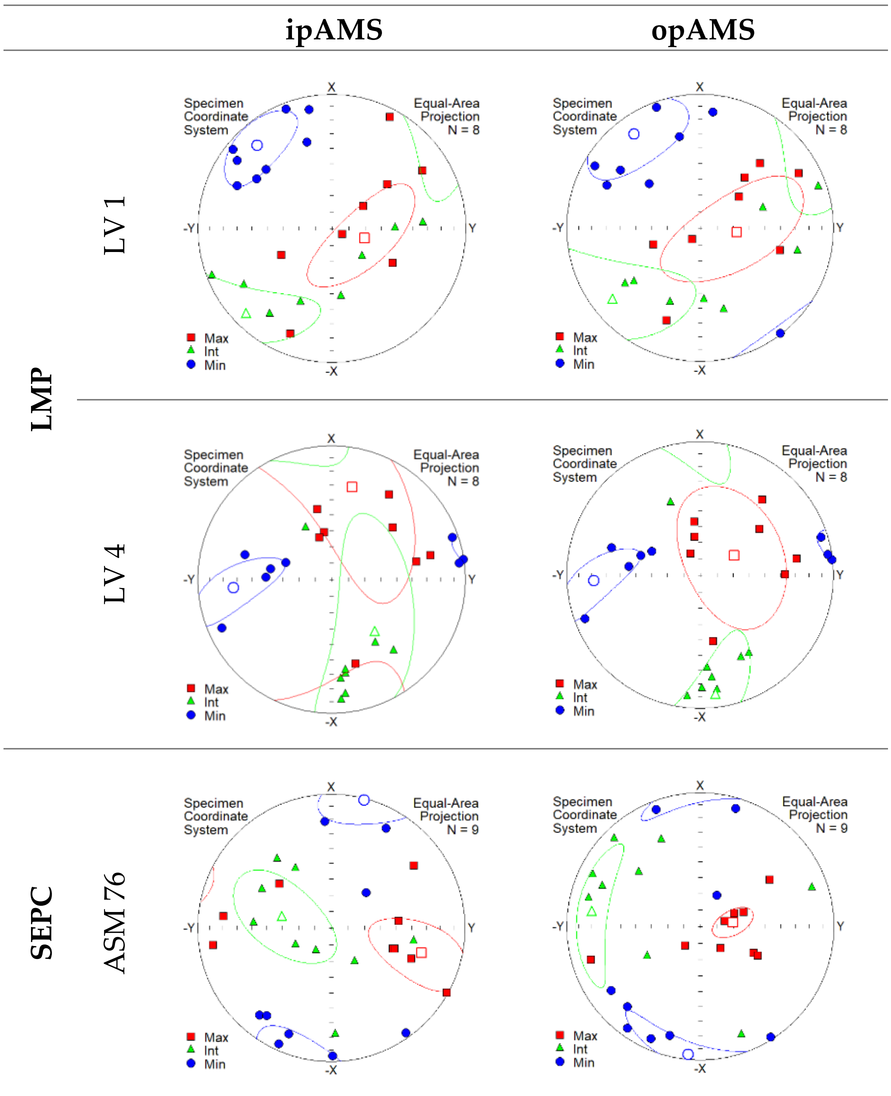

Figure 5. ipAMS and opAMS mean tensors for LMP and SEPC sub-samples, according to specimen coordinate system, and 95% confidence areas. Equal-area projection, lower hemisphere (the hollow symbols represents the corresponding mean vectors).

5. Conclusions

In conclusion, as the out-of-phase susceptibility is only non-zero in some minerals, the opAMS of rocks containing these minerals can be used as a tool for the direct determination of the magnetic subfabrics of these minerals. It should be noted that the opAMS indicated similar conclusions to studies on anisotropy of anhysteretic remanent magnetization (AARM) (e.g., [7]), as both are related to the presence of ferromagnetic minerals and their magnetic properties (e.g., magnetite and titanomagnetite). However, the opAMS does not require the permanent magnetization of samples and is measured simultaneously with the ipAMS.

Our studies prove that in plutons composed of magnetite-type granites, where both ferromagnetic and paramagnetic minerals are present, the magnetic fabric is, in most cases, coaxial. The coaxiality proves that the magnetite and/or hematite subfabric tends to have the same orientation as the other minerals in the matrix, namely the biotite. The non-coaxiality verified in sample LM 39 may be due to several factors, such as the magnetic susceptibility of this sample being very low, which leads to a greater inaccuracy of the measurements; it should be noted that this technique works better on rocks with high magnetic susceptibilities. Nevertheless, the results obtained for these granites, even in samples with lower magnetic susceptibility values, are satisfactory.

Author Contributions: Conceptualization, C.C., H.S., W.M. and F.N.; methodology, C.C. and W.M.; software, C.C. and W.M.; validation, C.C., H.S., W.M. and F.N.; formal analysis, C.C., H.S., W.M. and F.N.; investigation, C.C., H.S., W.M. and F.N.; resources, C.C. and W.M.; data curation, C.C., H.S., W.M. and F.N.; writing—original draft preparation, C.C. and W.M.; writing—review and editing, C.C., H.S., W.M. and F.N.; visualization, C.C., H.S., W.M. and F.N.; supervision, H.S. and F.N.; project administration, H.S.; funding acquisition, C.C. All authors have read and agreed to the published version of the manuscript.

Funding: The first author is a contracted researcher under the UIDP/04683/2020 project (Fundação para Ciência e a Tecnologia- Portugal). This work was partially funded by the Fundação para a Ciência e a Tecnologia under the UIDB/04683/2020 project.

Data Availability Statement: Not applicable.

Acknowledgments: The authors are grateful to the reviewers whose comments greatly helped to improve the manuscript.

Conflicts of Interest: The authors declare no conflict of interest.

References

1. Ferré, E.C. Theoretical models of intermediate and inverse AMS fabrics. *Geophys. Res. Lett.* **2002**, *29*, 1127. [CrossRef]
2. Hrouda, F.; Jelinek, V. Resolution of ferromagnetic and paramagnetic anisotropies, using combined low-field and high-field measurements. *Geophys. J. Int.* **1990**, *103*, 75–84. [CrossRef]
3. Rochette, P. Magnetic susceptibility of the rock matrix related to magnetic fabric studies. *J. Struct. Geol.* **1987**, *9*, 1015–1020. [CrossRef]
4. Martín-Hernandez, F.; Hirt, A.M. A method for the separation of paramagnetic, ferrimagnetic and haematite magnetic subfabrics using high-field torque magnetometry. *Geophys. J. Int.* **2004**, *157*, 117–127. [CrossRef]
5. Ferré, E.C.; Martín-Hernández, F.; Teyssier, C.; Jackson, M. Paramagnetic and ferromagnetic anisotropy of magnetic susceptibility in migmatites: Measurements in high and low fields and kinematic implications. *Geophys. J. Int.* **2004**, *157*, 1119–1129. [CrossRef]
6. Román-Berdiel, T.; Casas, A.M.; Oliva-Urcia, B.; Pueyo, E.L.; Liesa, C.; Soto, R. The Variscan Millares granite (central Pyrenees): Pluton emplacement in a T fracture of a dextral shear zone. *Geodin. Acta* **2006**, *19*, 197–211. [CrossRef]
7. Raposo, M.I.B.; Gastal, M.C.P. Emplacement mechanism of the main granite pluton of the Lavras do Sul intrusive complex, South Brazil, determined by magnetic anisotropies. *Tectonophysics* **2009**, *466*, 18–31. [CrossRef]
8. Oliva-Urcia, B.; Larrasoaña, J.C.; Pueyo, E.L.; Gil, A.; Mata, P.; Parés, J.M.; Schleicher, A.M.; Pueyo, O. Disentangling magnetic subfabrics and their link to deformation processes in cleaved sedimentary rocks from the Internal Sierras (west central Pyrenees, Spain). *J. Struct. Geol.* **2009**, *31*, 163–176. [CrossRef]
9. Martín-Hernández, F.; Ferré, E.C. Separation of paramagnetic and ferrimagnetic anisotropies: A review. *J. Geophys. Res.* **2007**, *112*, B03105. [CrossRef]
10. Hrouda, F.; Pokorný, J.; Jezek, J.; Chadima, M. Out-of-phase magnetic susceptibility of rocks and soils: A rapid tool for magnetic granulometry. *Geophys. J. Int.* **2013**, *194*, 170–181. [CrossRef]
11. Hrouda, F.; Chadima, M.; Jezek, J.; Pokorný, J. Anisotropy of out-of-phase magnetic susceptibility of rocks as a tool for direct determination of magnetic subfabrics of some minerals: An introductory study. *Geophys. J. Int.* **2017**, *208*, 385–402. [CrossRef]
12. Hrouda, F.; Chadima, M.; Ježek, J.; Kadlec, J. Anisotropies of in-phase, out-of-phase, and frequency-dependent susceptibilities in three loess/palaeosol profiles in the Czech Republic; methodological implications. *Stud. Geophys. Geod.* **2018**, *62*, 272–290. [CrossRef]
13. Hrouda, F.; Chadima, M.; Ježek, J. Anisotropy of Out-of-Phase Magnetic Susceptibility and Its Potential for Rock Fabric Studies: A Review. *Geosciences* **2022**, *12*, 234. [CrossRef]
14. Hrouda, F. Magnetic anisotropy of rocks and its application in geology and geophysics. *Geophys. Surv.* **1982**, *5*, 37–82. [CrossRef]
15. Tarling, D.H.; Hrouda, F. *The Magnetic Anisotropy of Rocks*; Chapman & Hall: London, UK, 1993; p. 217.
16. Jackson, M. Imaginary susceptibility, a primer. *IRM Q.* **2004**, *13*, 10–11.
17. Sant'Ovaia, H.; Ribeiro, M.A.; Martins, H.C.B.; Ferrão, F.; Gomes, C.; Noronha, F. Estruturas e fabric magnético no maciço granítico de Lavadores-Madalena. *Comun. Geol.* **2014**, *101*, 313–317.
18. Cruz, C.; Sant'Ovaia, H.; Noronha, F. Magnetic mineralogy of Variscan granites from northern Portugal: An approach to their petrogenesis and metallogenic potential. *Geol. Acta* **2020**, *18*, 1–20. [CrossRef]
19. Dias, J.M.; Cruz, C.; Sant'Ovaia, H.; Noronha, F. Assessing the Magnetic Mineralogy of the Pre-Variscan Manteigas Granodiorite: An Unexpected Case of a Magnetite-Series Granitoid in Portugal. *Minerals* **2022**, *12*, 440. [CrossRef]

20. Sant'Ovaia, H.; Nogueira, P.; Carrilho Lopes, J.; Gomes, C.; Ribeiro, M.A.; Martins, H.C.B.; Dória, A.; Cruz, C.; Lopes, L.; Sardinha, R.; et al. Building up of a nested granite intrusion: Magnetic fabric, gravity modelling and fluid inclusion planes studies in Santa Eulália Plutonic Complex (Ossa Morena Zone, Portugal). *Geol. Mag.* **2015**, *152*, 648–667. [CrossRef]
21. Cruz, C.; Sant'Ovaia, H.; McCarthy, W.; Noronha, F. Anisotropy of out-of-phase magnetic susceptibility: A non-standard approach for magnetic subfabrics determination. In Proceedings of the X CJIG LEG 2020, Estremoz, Portugal, 20–22 November 2020.
22. Terrinha, P.; Pueyo, E.L.; Aranguren, A.; Kullberg, J.C.; Kullberg, M.C.; Casas-Sainz, A.; Azevedo, M.R. Gravimetric and magnetic fabric study of the Sintra Igneous complex: Laccolith-plug emplacement in the Western Iberian passive margin. *Int. J. Earth Sci.* **2018**, *107*, 1807–1833. [CrossRef]
23. Román-Berdiel, T.; Aranguren, A.; Cuevas, J.; Tubia, J.M. Compressional granite-emplacement model: Structural and magnetic study of the Trives Massif (NW Spain). *Lithos* **1998**, *44*, 37–52. [CrossRef]
24. Pueyo, E.L.; Román-Berdiel, T.; Calvín, P.; Bouchez, J.L.; Beamud, E.; Ayala, C.; Loi, F.; Soto, R.; Clariana, P.; Margalef, A.; et al. Petrophysical Characterization of Non-Magnetic Granites; Density and Magnetic Susceptibility Relationships. *Geosciences* **2022**, *12*, 240. [CrossRef]
25. Ishihara, S. The Magnetite-series and Ilmenite-series Granitic Rocks. *Min. Geol.* **1977**, *27*, 292–305.
26. Chadima, M.; Pokorny, J.; Studynka, J. *Safyr7: Kappabridge Control Software (for windows)*; AGICO, Inc.: Brno, Czech Republic, 2018.
27. Jelinek, V. Characterization of the magnetic fabric of rocks. *Tectonophysics* **1981**, *79*, T63–T67. [CrossRef]
28. Franke, W. Variscan plate tectonics in Central Europe–current ideas and open questions. *Tectonophysics* **1989**, *169*, 221–228. [CrossRef]
29. Ribeiro, A.; Pereira, E.; Dias, R. Structure in the Northwest of the Iberian Peninsula. In *Pre-Mesozoic Geology of Iberia*; Dallmeyer, R.D., Martínez Garcia, E., Eds.; Springer: Berlin/Heidelberg, Germany, 1990; pp. 220–236.
30. Kroner, U.; Romer, R.L. Two plates-Many subduction zones: The Variscan orogeny reconsidered. *Gondwana Res.* **2013**, *24*, 298–329. [CrossRef]
31. Julivert, M.; Fontboté, J.M.; Ribeiro, A.; Conde, L. *Mapa tectónico de la península Ibérica y Baleares a escala 1:1,000,000 y memoria explicativa*; Instituto Geologico y Mineiro de España: Madrid, Spain, 1974.
32. Pereira, M.F.; Apraiz, A.; Silva, J.B.; Chichorro, M. Tectonothermal analysis of high-temperature mylonitization in Coimbra-Cordoba shear zone (SW Iberian Massif, Ouguela tectonic unit, Portugal): Evidence of intra-continental transcurrent transport during the amalgamation of Pangea. *Tectonophysics* **2008**, *461*, 379–394. [CrossRef]
33. Pereira, E. *Notícia Explicativa da Folha 10-A (Celorico de Basto) da Carta Geológica de Portugal: 1:50 000*; Serviços Geológicos de Portugal: Lisboa, Portugal, 1989; p. 53.
34. Helal, B. Granitoïdes, Granites à Métaux Rares et Hydrothermalisme Associe: Géologie, Minéralogie et Géochimie de Plusieurs Suites Tardi-Hercyniennes (Nord du Portugal). Ph.D. Thesis, Ecole Nacionale Superieure des Mines de Saint-Etienne, Saint-Étienne, France, 1992.
35. Fernandes, S.; Gomes, M.; Teixeira, R.; Corfu, F. Geochemistry of biotite granites from the Lamas de Olo Pluton, northern Portugal. In Proceedings of the Geophysical Research Abstracts, EGU General Assembly, Vienna, Austria, 7–12 April 2013.
36. Cruz, C.; Góis, J.; Sant'Ovaia, H.; Noronha, F. Geostatistical approach in the study of the magnetic susceptibility variation: Lamas de Olo Pluton case study. *J. Iber. Geol.* **2020**, *46*, 279–289. [CrossRef]
37. Cruz, C.; Sant'Ovaia, H.; Noronha, F. Magnetic susceptibility and $\delta^{18}O$ characterization of Variscan granites related to W-(Mo) and Sn-(W) mineralizations: Lamas de Olo Pluton case study. *Comun. Geol.* **2016**, *103*, 143–147.
38. Martins, H.C.B.; Sant'Ovaia, H.; Abreu, J.; Oliveira, M.; Noronha, F. Emplacement of Lavadores granite (NW Portugal): U/Pb and AMS results. *Comptes Rendus Geocience* **2011**, *343*, 387–396. [CrossRef]
39. Cruz, C.; Roseiro, J.; Martins, H.C.B.; Nogueira, P.; Sant'Ovaia, H. Magmatic sources and emplacement mechanisms of the Santa Eulália Plutonic Complex facies: Integrating geochronological and geochemical data. In Proceedings of the Geoquímica Ibérica: Compendio de los trabajos presentados en el XIII Congreso Nacional de Geoquímica y XIII Congreso Ibérico, Puertollano, Spain, 25–27 April 2022; pp. 223–231.